AD NUMBER
AD313752
CLASSIFICATION CHANGES
TO: unclassified
FROM: confidential
LIMITATION CHANGES
TO: Approved for public release, distribution unlimited
FROM:
AUTHORITY
OCA; DoD Dir 5200.20, 28 Jul 77; ONR ltr 28 Jul 77

CONFIDENTIAL

AD 313 752

FOR MICRO-CARD CONTROL ONLY

1 OF 2

Reproduced by

Armed Services Technical Information Agency

ARLINGTON HALL STATION; ARLINGTON 12 VIRGINIA

CONFIDENTIAL

CONFIDENTIAL

MASSACHUSETTS INSTITUTE OF TECHNOLOGY
NAVAL SUPERSONIC LABORATORY

Technical Report 227

(Unclassified Title)

SIGNALS FROM AERODYNAMICALLY HEATED INFRARED DOMES AND SPIKES

Fourth Quarterly Progress Report
Contract AF 33(616)-3909
August, September, October, 1957

Technical Report 227
Contract Nonr 1841(40)
October 1957

CONFIDENTIAL

CONFIDENTIAL

Massachusetts Institute of Technology
Naval Supersonic Laboratory
Cambridge 39, Massachusetts

Technical Report 227

(Unclassified Title)

SIGNALS FROM AERODYNAMICALLY HEATED INFRARED DOMES AND SPIKES

by

Myron J. Block

Fourth Quarterly Progress Report
Contract AF 33(616)-3909
August, September, October, 1957

Technical Report 227
Contract Nonr 1841(40)
October 1957

This report contains vii
and 59 pages. Copy No. 64
of 75 copies.

NSL Log 3516

SUMMARY

Methods are given for calculating the effective infrared radiation from aerodynamically heated windows or spikes. The radiation generally has a time-varying component due either to non-uniform irradiation of the chopping reticle or from looking at various parts of the heated window or spike due to scanning or tracking operations. This time-varying radiation at the detector is shown to be generally tolerable if the scanning frequency is made small compared with the operating frequencies passed by the amplifying system.

INTRODUCTION

In a missile with an infrared detection system in its nose aerodynamic heating will cause the protective window (IR dome) to irradiate the detector. In flight at high mach numbers, the radiation from the window, called a "false signal", may completely mask the signal from the target. In such cases, some method must be found to reduce the window radiation. One possibility is to replace the window by a narrow spike as suggested in Ref. 1. The spike separates the flow over the front of the missile reducing both the aerodynamic drag and heating. The spike, however, will become hot and radiate. This report deals with the radiation from the IR dome in Part I and with the spike radiation in Part II. It is assumed that the temperature distribution on the spike or window is known. Temperatures are calculated for several cases in Ref. 2 for example. In this present report, methods are given for calculating the radiation reaching the detector from heated windows and spikes.

TABLE OF CONTENTS

TABLE OF CONTENTS (Concluded)

LIST OF ILLUSTRATIONS

PART I
RADIATION FROM IR DOMES

A. INTRODUCTION

This part of the report deals with the signals which are received by the detector due to the aerodynamic heating of different types of windows. In each case we have considered that the window is used to protect a Sidewinder type IR system (Ref. 3).

The Sidewinder type system considered consists of a folded optical system having a primary mirror which receives radiation and reflects it to a secondary plane mirror where it is reflected and sent through a reticle pattern (chopper) onto the surface of a detector (Fig. 1). The field of view of this system at any instant is three degrees and the total rotation of the optical system is plus or minus 20 degrees from the missile axis. In this geometry, the secondary mirror, itself, acts as a mask blocking out the center of the incoming radiation field.

B. FALSE SIGNAL FROM A HEMISPHERICAL WINDOW

The window radiation at the detector will have, in general, a time dependent part superimposed on a steady background level. Since the non varying ("DC") level will not be passed by the amplifiers in the detecting system, its effect will be only to raise the background noise of the detecting cell thus reducing its overall sensitivity. This problem has been treated in detail in Ref. 4. We will now consider the time-varying part of the window radiation.

The time-dependent irradiation at the detector may be generated by the heated window in a number of ways depending on the seeker system. The Sidewinder type system looks through different parts of its window as it tracks. If the window is at a uniform temperature then no unsteady false signal will be generated by the tracking motion since equal window area is always seen. When the window is not at a uniform temperature, false signals can be produced in several ways which will be separately analysed in the following sections.

1. False Signal From Non-Uniform Irradiation of Chopper

If the window radiation produces a time-independent, but non-uniform irradiation on the chopper, then a false signal can be produced at frequencies which are harmonic of the chopping frequency.

For any given position of the optical system the window can be divided into three parts. One part will produce no irradiation of the chopper and hence no false signal. Another portion will produce irradiation of the chopper which is symmetrical about the chopper axis and which, therefore, will produce no false signal. The remaining small portion of the window can irradiate the chopper non-symmetrically and can, therefore, result in a false signal.

According to Ref. 4, the irradiation of the reticle is symmetrical about the optical axis, providing the radiating surface is within the volume formed by rotating areas A and B (in Fig. 2) about the "y" axis. The radiation that is emitted within the two 3" annuli, whose sections are given by C, F and D, E, respectively, is also received on the recticle but non-uniformly. We shall call these the "non-u" annuli. In section C, for instance, the radiation from a point on the extreme left irradiates only one edge of the reticle. As the radiating point moves to the right more of the reticle is illuminated until, as we move into region A, the reticle is symmetrically illuminated.

When the irradiation of the reticle is non-symmetrical, the spinning of the reticle will modulate some fraction of the flux at the chopping frequency. Thus, while the total amount of such non-symmetrical irradiation is small, it may be modulated to the frequencies which the detecting system readily accepts.

As the "non-u" annuli sample radiation around all the boundaries of the annulus A, B, we may assume that the average intensity of radiation is the same, and that the ratio of the total radiation from the non-u annuli to that from A,B is in proportion to the projected area of the window in them. (For the hemispherical window there is a small effect due to changing effective thickness of the window which has been neglected here). Therefore

$$\frac{\phi_{non-u}}{\phi_{AB}} = \frac{3\pi}{180} D \frac{(2\pi R_1 + 2\pi R_2)}{\pi R_2^2 - \pi R_1^2} = 0.078 \qquad (1)$$

where D is the distance to the mirror, and R_1 and R_2 are illustrated in Fig. 2.

The amplitude of the modulated radiation is less than the total irradiation from the "non-u" annuli. There are two important types of radiation distribution on these annuli which result in no modulation whatsoever. If certain symmetries exist in the radiation from the "non-u" annuli, then to first order there is a uniform irradiation of the reticle and no modulation. If equal radiators are placed in the pair of positions M and N marked below, this situation holds

<u>M</u>	<u>N</u>
a distance, x, from the left edge of C	a distance, x, from the left edge of F
a distance, x, from the left edge of D	a distance, x, from the left edge of E

More important is the case of the radiation pattern on the window which is cylindrically symmetric with respect to the optical axis. In this case the irradiation of the detector is also cylindrically symmetric and there is no modulation.

2. False Signal Due to Motion of Optical System with Respect to Missile Window

In tracking or searching when the aperture scans across the radiation non-uniformities on the window, the detector sees a false signal whose frequency is some function of the scanning rate. In this manner a false signal might be produced that has a harmonic at the chopping frequency.

Owing to the geometry of the folded mirror system, radiation from the target passes through an annulus of the window, centered on the optical axis. The optical axis is free to move ± 20° with respect to the axis of the missile, in tracking a target. We calculate here the radiation from the annulus incident on the detector where there is relative motion between the optical system and the window.

The hemispheric effective radiation from points on the window has been calculated, based on the temperature distribution of Fig. 3 (from Ref. 2) for flight at M = 3.5, and at an altitude of 50,000 feet. The radiation distribution is symmetric about the direction of motion of the missile. In Fig. 4, this distribution has been plotted. If φ is the polar angle with respect to the direction of motion, the hemispheric radiation is well represented by the form

$$j_0(\varphi) = (0.0017 + 0.0012 \cos \varphi) \text{ effective watts/cm}^2 \quad (2)$$

These figures correspond to a window thickness of 5 mm. and include the effect of window (quartz) emissivity and spectral response of the detector (uncooled PbS cell).

Let θ be the vectorial angle between the axis of the optical system and an arbitrary point P on the window, and let α be the vectorial angle between the optical axis and the axis of the temperature distribution (see Fig. 5). Then, if φ is the angular coordinate of P with respect to the temperature axis, we have

$$\alpha + \theta = \varphi \quad (3)$$

Now consider the radiation from an element of area dA at P (within the annulus) into the chopper. Let $d\Omega$ be the solid angle subtended by the chopper (as seen through the optics) at P. Since the chopper is in the focal plane of the optical system, $d\Omega$ is constant for all points of the annulus and is equal to the solid angle of the field of view seen by the chopper.

The projection of dA normal to the line of sight to the detector is dA cos θ. Hence the radiation from dA into the detector is

$$dS = \frac{d\Omega}{\pi} j_0 (\psi) \cos\theta \, dA \tag{4}$$

If θ_1 and θ_2 represent the polar angular limits of the annulus, then the total radiation from the annulus incident on the detector is

$$S = R^2 \frac{d\Omega}{\pi} \int_0^{2\pi} d\phi \int_{\theta_1}^{\theta_2} \sin\theta \cos\theta \, j_0 (\psi) \tag{5}$$

where ϕ is the azimuth of the point P with respect to the optical system of coordinates. Introducing Eqs. (2) and (3) we obtain

$$S = \frac{R^2 d\Omega}{\pi} \int_0^{2\pi} d\phi \int_{\theta_1}^{\theta_2} \sin\theta \cos\theta \, d\theta \left[a + b\left\{\cos\theta \cos\alpha + \sin\theta \sin\alpha \cos(\phi - \phi')\right\}\right] \tag{6}$$

where ϕ' is the azimuthal angle of the temperature axis with respect to the optical system of coordinates, and where $a = 0.0013$, $b = 0.0012$. The term involving ϕ' vanishes on integration. The remaining terms are integrated to yield

$$S = 2R^2 \, d\Omega \left\{\frac{a}{2} (\sin^2\theta_2 - \sin^2\theta_1) + \frac{b}{3} \cos\alpha (\cos^3\theta_1 - \cos^3\theta_2)\right\} \tag{7}$$

$$= A + B \cos\alpha \tag{8}$$

the coefficients A and B being defined by the above relation.

The constants for the Sidewinder system have been taken as follows:

$2R = 12.5$ cm.
$d\Omega = 1.71 \times 10^{-4}$ sterad
$\theta_1 = 19.2°$
$\theta_2 = 46.1°$

The coefficients A and B may then be computed as

$$A = 3.58 \text{ microwatts}$$
$$B = 2.53 \text{ microwatts} \tag{9}$$

The Fourier spectrum of the false signal depends on the behavior of the angle α. For a linear variation of angle of attack ($\dot{\alpha}$ = const) Eq. (7) is already a Fourier series. The maximum track rate for the assumed system is 30°/sec (Ref. 3); this corresponds to a frequency of 1/12 cps. Since the Sidewinder electronics system has a passband at 1500 - 2000 cps, it is reasonable to assume that this false signal is of negligible importance.

We may therefore conclude that the false signal due to tracking through various parts of the hemisphere is negligible. This result is a consequence of the fact that the tracking rate is so much smaller than the chopping frequency.

3. False Signal from a Linear Irradiation Distribution

Assume that the irradiation on the reticle is a linear function of the distance, x, along a space-fixed axis in the reticle plane (see Fig. 6)

$$\phi = \phi_M \left(\frac{r}{d} \cos\theta + \frac{1}{2} \right) \tag{10}$$

where d = diameter of reticle, r = distance from center of reticle, θ = polar angle, ϕ_M = maximum irradiation of detector.

The transparent sections of the reticle have θ boundaries given by

$$\theta_i = \frac{\pi}{25} i + 60 \pi t \quad (i = 0, \ldots 24)$$

and r boundaries

$$r_j = r_1 \sqrt{j} \qquad (j = 1, \ldots 13)$$

Thus the signal falling on the detector is

$$S = \phi_M \sum_{i=0}^{24} \int_{\theta_i}^{\theta_{i+1}} d\theta \int_R dr \left(\frac{r \cos\theta}{d} + \frac{1}{2} \right) r$$

where R stands for the regions for r in the zone θ_i, θ_{i+1}

$$S = \phi_M \sum_{i=0}^{24} \int_R dr \left[-\frac{r^2}{d} \sin\left\{\frac{\pi}{25}(i+1) + 60\pi t\right\} \right.$$

$$\left. + \frac{r^2}{d} \sin\left\{\frac{\pi}{25} i + 60\pi t\right\} + \frac{\pi r}{50} \right] < \phi_M \frac{A}{2} \qquad (11)$$

where ϕ is the reticle area.

The modulation is thus of only 30 c/s frequency. The response of the system for this frequency is small. Remembering that the radiation from the "non-u" annuli is $\sim$0.078 of that from the main annulus, we have, for an unprotected hemispherical window (M = 3.5, at 30,000 feet)

$$\phi < 3 \times 10^{-7} \text{ A watts}$$

We have here considered ϕ_M to be the whole amplitude from the "non-u" annuli. As previously noted the cylindrically symmetrical component does not contribute. As the value of ϕ is already negligible we shall only make a rough estimate of the further reduction factor due to cylindrical asymmetry. The non-cylindrical asymmetry for a 20° angle of attack may be considered to be due to sampling by opposite sides of the optical system from the hot and cool halves of the window respectively. As discussed in a later section, this amounts to about 1/5th asymmetry. This reduces ϕ to

$$\phi < 6 \times 10^{-8} \text{ A watts}$$

4. False Signal from a Step Irradiation Distribution

The radiation from a small source may tend to illuminate one portion of the reticle and not the remainder, leaving a sharp boundary between the two regions. The boundary line may be expected to be smooth and have few "wiggles" over the reticle face. This case may also be considered to put an upper bound on the effect of window radiation. The radiation may not lead to a pattern as smooth as the linear pattern assumed above, but will certainly lead to a much smoother pattern than the step function assumed now.

In Fig. 7 curve p is an illustration of the type of boundary curve required to modulate, at a 750 cycle frequency, the radiation falling on 1/50th of the reticle. It is so irregular and "wiggly" as to be extremely improbable. On the other hand, Q is a very likely boundary curve, but it modulates the radiation falling on one of the open areas only, 1/300th of the reticle area. It is easily seen that any curve, modulated at 750 c/s, must have sharp wiggles to modulate a greater fraction of the ir radiation than this. Straight lines cutting more than one open area do so in such a way that the different areas compensate each other as the reticle spins. Modulations of greater amounts of radiation can be obtained but at frequencies of $\frac{750\ c/s}{n}$ (n an integer > 1). As the frequency response of the detector is critical we may concentrate our attention on the 750 c/s modulation. Then

$$\phi = \frac{\phi_M}{300}$$

If the window produces a step-like irradiation of the reticle it must be due to a small area of the window, acting approximately as a point source. At M = 3.5 and h = 50,000 feet the radiation from a point on the window will not exceed $\phi_M = 10^{-9}$ A watts.

C. FALSE SIGNAL FROM A CONICAL WINDOW

As has been shown, there are two types of time dependent irradiation of the detector, the type that is independent of the chopper and the type that is produced by the chopper. The first arises from the chopper being uniformly and time dependently irradiated. The second arises from the time independent non-uniform irradiation of the chopper.

The detector and amplifier system considered has a sensitivity to radiation depending upon the modulation frequency of the radiation incident upon the detector. The sensitivity is greatest for the chopper frequency f_0. The ratio of the amplitude of the system output for radiation modulated sinusoidally at a frequency f to the amplitude for sinusoidal modulation at frequency f_0 is called the relative response, r_f, of the system at frequency f. The relative response may be approximated by a Gaussian distribution:

$$r_f = e^{-\left(\frac{f - f_0}{\Delta}\right)^2} \tag{12}$$

where the constant Δ determines the width of the distribution.

Let us consider only the window radiation which irradiates the reticle symmetrically. Due to the symmetry of the irradiation the reticle does not modulate this irradiation. Thus there will only be a false signal if the window spike radiation received by the annulus is time dependent.

Such a time dependence may be obtained from changing temperature distributions on the window, or from the scanning of the optical system over different portions of the window. The former occurs at a very slow rate, and may be neglected if the latter is shown to be unimportant.

We shall concern ourselves with a harmonic scanning of 20° amplitude and a frequency, f_s of 5 c/s.

1. The Fourier Analysis

Let $\phi(t)$ be the irradiation of the detector as a function of time, t.

If $\phi(t)$ is a periodic function of time with period f_s^{-1}, then it may be analyzed into a Fourier series:

$$\phi(t) = \frac{1}{2} \Phi_e(0) + \sum_{n=1}^{\infty} \left[\Phi_0(n) \sin 2\pi f_n t + \Phi_e(n) \cos 2\pi f_n t \right] \tag{13}$$

where $f_n = nf_s$

$$\Phi_{\substack{o\\e}}(n) = 2 f_s \int_0^{f_s^{-1}} dt\, \phi(t) \begin{Bmatrix} \sin \\ \cos \end{Bmatrix} 2\pi f_n t$$

$$= 2 \int_0^1 dK\, \phi'(K) \begin{Bmatrix} \sin \\ \cos \end{Bmatrix} 2\pi n K \qquad (14)$$

where $K = f_s t$, $\phi'(K) = \phi(t)$

and the subscripts "o" and "e" represent the odd and even Fourier components of $\phi(t)$ respectively.

If $\phi(t)$ is not periodic, but is transient, then the above analysis into a Fourier series must be replaced by a Fourier transform. The cases treated will be periodic. The conclusions obtained will be valid for transients also.

2. Effective Irradiation

If we assume that the detector and amplifier system is linear (response to two simultaneous signals is the sum of the responses which each signal alone would produce) then we may consider the response to each frequency component separately. Since r_f is small unless f is near f_o, the response will be negligible except for such frequencies. The amplitude of the component of $\phi(t)$ having frequency f_r is

$$\sqrt{\Phi_o^2(n) + \Phi_e^2(n)}$$

The system response to this component will have a certain amplitude; if irradiation of amplitude

$$R_n = r_{f_n} \sqrt{\Phi_o^2(n) + \Phi_e^2(n)}$$

and frequency f_o irradiated the detector, the system response would be the same. Thus, in this sense, R_n is the effective radiation corresponding to the component of $\phi(t)$ of frequency f_n. Then we can define the effective irradiation corresponding to $\phi(t)$ as

$$R = \sum_{n=1}^{\infty} R_n \tag{15}$$

3. The Flux $\phi(t)$ from a Conical Window

We will now consider the case of a conical window. We see from Figs. 19, 21, 22 and 23 of Ref. 4 that the radiation from the cone varies smoothly, and approximately linearly with the height coordinate of the cone. The flux accepted by the annulus will vary even more smoothly with the orientation of the optical axis than the curves, because the annulus integrates large portions of the curve. The annulus accepts radiation from about one half the window at any instant.

In general, when the optical axis moves off the missile axis one part of the annulus moves to cooler regions, while the opposite part moves to hotter regions, tending to compensate. We shall ignore this however and use for the amplitude of flux variation, ϕ_M, the difference in irradiation obtained by integrating first over the warmer half of the above mentioned curves, and secondly over the cooler halves.

Examining Figs. 19 and 21 (of Ref. 4) we obtain ϕ_M to be approximately 0.2 of the total radiation for the cone at 20° attack angle. From Figs. 22 and 23 we obtain ϕ_M to be approximately 0.5 of the total radiation for the cone at 0° attack angle. Thus the maximum value of ϕ_M for the given values of attack angle, Mach number and altitude, is approximately

$$\phi_M = 0.6 \times 10^{-4} \text{ watts/cm}^2 \text{ for } M = 3.5,\ h = 30{,}000$$

and a 20° angle of attack.

If we consider the variation in $\phi(t)$ with angle to be linear, but the optical system to be scanning harmonically, we have

$$\phi(t) = -\phi_M \left| \sin 2\pi f_s t \right| + \phi_{steady} \tag{16}$$

The absolute value signifies that the temperature drops as the optical axis passes the cone axis from any direction. This is in fact a derivative discontinuity which in practice is smoothed over. Thus we may expect that the high frequency components we get are exaggerated and we over-estimate the detector response R.

Combining Eqs. 14 and 16,

$$\Phi_c(n) = -4\phi_M \int^{\frac{1}{2}} |\sin 2\pi K| \cos 2\pi n K \ dK$$

$$= -2\frac{\phi_M}{\pi}\begin{cases} \frac{1}{n+1} - \frac{1}{n-1} & n = \text{even} \\ 0 & n = \text{odd} \end{cases}$$

while $\Phi_s(n) = 0$

Therefore

$$R_n = \begin{cases} \frac{4\, r_n}{\pi (n^2-1)} \phi_M & n = \text{even} \\ 0 & n = \text{odd} \end{cases}$$

and

$$R = \frac{4\phi_M}{\pi} \sum_{n=\text{even}} \frac{r_n}{n^2-1}$$

For example, if $f_s = 5$ c/sec., $f_0 = 750$ c/sec., $\Delta = 189$ c/sec. (where this value for Δ corresponds to a 3 db loss at 100 c/sec. from f_0) we have

$$R = \phi_M K \qquad 0.6 \times 10^{-3} < K < 10^{-3}$$

Thus the effective irradiation from the window is less than 0.6×10^{-7} watts/cm²

D. CONCLUSIONS

The expected false signals calculated here are reasonably small compared with a target signal $> 10^{-6}$ effective watts/cm².

If the false signal here calculated is still too large for certain desired target signals a remedy would be to sharpen the response curve of the detector. At present $r_f \approx 1/10$ for $|f - f_0| = 300$ c/s. Thus the detector system passes a large fraction of those components of frequencies which are only sixty times greater than f_s and only 15 times greater than f_q. This is serious for step function type curves which decrease only inversely as the multiple n. Decreasing the width of r_f has the effect of decreasing the number of multiples n of f_s or f_q in the pass band. Note that we are assuming a uniform sensitivity over the detector surface.

PART II
RADIATION FROM SPIKES

A. INTRODUCTION

Previously, (Ref. 4), the effect of aerodynamically heated windows irradiating their detectors has been computed for certain temperature distributions on conical and hemispherical windows. The use of a cone reduces the irradiation compared with that from a hemisphere, when the cone is at 0° attack angle due to the lower temperatures on the cone.

Because the cone has less aerodynamic drag and is heated to a somewhat lower temperature than the hemisphere, it is to be preferred. However in using a conical window, the temperature reduction may not be great enough to justify the cost and loss in optical resolution. Compromise shapes such as pyramids with hemispherical tips have been suggested but such shapes will irradiate their detectors more intensely than a cone.

In order to effect a more substantial decrease in detector irradiation, prevent image quality deterioration, and yet maintain the low drag of the cone, the use of a spike has been proposed to replace the window, (Ref. 1). A protective window (probably hemispherical) could be used with the spike to reduce air currents. However because of the presence of the spike the temperatures on the protective window will be reduced below those on the original window. The spike reduces the pressure loading on the window so that a thinner shell may be used. Since the window intensity is approximately proportional to its thickness, a thin hemispherical protective window would irradiate the detector less, even at the same temperature than a thicker hemispherical window. However, the spike itself is heated aerodynamically and as it is seen by the optical system at certain times it introduces a new series of problems. We will therefore evaluate the effects of a spike-window on a Sidewinder type detection system.

B. SPIKE POSITION WITH RESPECT TO THE OPTICAL SYSTEM

A realistic length of a spike for the assumed Sidewinder type design would be 5.5". Figure 8 with a line drawn out to point A shows the position of the proposed spike on axis. Instead of rotating the optical system with respect to the spike, as it would happen in practice, the analysis is simplified by moving the spike around the pivot point. In principle, one should also rotate the window, but the edges of the window will not cut off any of the radiation and, consequently, this was not done. Spike positions B, B', C, and C' represent rotations of the system through 5.5 degrees, 7.5 degrees, 10.5 degrees, and 13.5 degrees respectively.

A ray of light parallel to the axis, (axial ray), which is not masked by the secondary plane mirror, will strike the primary parabolic mirror and be focussed at the middle of the detector. The present optical design also allows that a ray at plus or minus 1.5 degrees from the axial ray will also be focussed onto the detector if it strikes the primary mirror.

Ray B is obtained by drawing a line to the edge of the secondary plane mirror mask at 1/2 degrees below the axial ray, the intersection of Ray B with the spike-position arc starting at point B. The line from point B to the center of the window represents the relative spike-optical system rotated 5.5 degrees. Ray B is the ray below which no part of the spike will be seen because of the effect of the secondary plane mirror mask.

Ray B' is drawn by starting at the edge of the plane mirror at 1/2 degrees above the axial ray. The line drawn between point B' and the pivot point represents the spike position for a system rotation of 7.5 degrees.

Ray C is drawn 1/2 degrees below that axial ray which intersects the outer edge of the primary mirror. Ray C' is 1/2 degrees above that same axial ray. The significance of these points is as follows:

1. No luminous point between Ray A and Ray B will be seen by the detector.

2. No luminous point above Ray C' will be seen because it is outside the field of view.

3. Every luminous point between Ray C and Ray B' will illuminate the detector symmetrically.

4. Points in the region between Ray B and Ray B' will illuminate the field asymmetrically.

5. Points in the region between Ray C and C' will also illuminate the field asymmetrically, but in the opposite direction from those between B and B'.

All masking will have no effect on the angular field, but it will affect the clear aperture.

The aerodynamically heated spike in positions 3, 4, and 5 will irradiate the infrared detection system. The purpose of this section is to evaluate the effects of the irradiations.

As we have shown previously, there is a range of spike positions in which the irradiation of the detection system is independent of spike positions. For any relative motion between the spike and the optical system within this range of positions, the consequent detector irradiation will be independent of time. As for relative motion beyond this range we may analyze the irradiation into time independent and time dependent components.

We will first consider the magnitude and the effects of the time independent irradiation of the detection system.

C. TIME INDEPENDENT COMPONENT

Consider a spike 0.5 cm in diameter. It may at times be at an angle such that its projection bridges the annular aperture shown in Fig. 8.

The maximum temperature of the spike will be no greater than that of the original hemispherical window. We will also assume that its maximum thickness (0.5 cm) is the same as that of the original hemisphere and that it has the same emissivity. Thus an upper limit on the irradiation of the detector by the spike will be obtained by multiplying the irradiation from the original hemispherical window by the ratio of the projected area of the spike to the area of the annulus.

$$\frac{\text{irradiation from spike}}{\text{irradiation from hemispherical window}} = \frac{0.5 \times 5}{\pi(7.5^2 - 2.5^2)} = 0.016$$

If we add a spike protruding from the front of the hemispherical window, then the resulting reduction in window temperature cuts its radiation to about 1/5 of its formed value. In addition, the use of the spike reduces the air loads so that if a sufficiently thin window can be used, then the window radiation can be further reduced to be equal to that from the spike. To achieve this reduction in window radiation, its thickness would have to be reduced to 1/12 that of the unprotected window.

The total irradiation will then be about 0.032 of the irradiation from the unprotected window; the latter being 2.1×10^{-4} watts/cm^2 for M = 3.5 and h = 50,000 ft.

Therefore it is estimated that the use of a spike even with a thin hemispherical window would reduce the time independent component of radiation. For example for flight at M = 3.5 at 50,000 ft. the irradiation is reduced by a factor of 0.03 to less than 10^{-5} watts/cm^2. The sensitivity of a PbS detector would thus be unaffected as its response is unaffected by background irradiations of less than 10^{-4} effective watts/cm^2.

D. TIME-DEPENDENT COMPONENT

In Part I of this report, a general expression was given relating the effective irradiation of the detector to the time dependent flux output from the window (or spike). We shall now estimate this irradiation for the case of the aerodynamically heated spike.

We have previously estimated the maximum flux received by the annulus from the spike. As the spike may be entirely out of view for part of the scanning period, we have

$$\varphi_M = 3.5 \times 15^{-6} \text{ watts/cm}^2$$

It is possible to conceive of the radiation coming from a small region near the tip of the spike. The total radiation is then likely to be less than that estimated above but we shall keep that as an upper bound.

In this case $\phi(t)$ will approximate a step function. The radiation will suddenly appear as the tip of the spike projects over the inner edge of the annulus, then vanish after it goes over the outer edge, etc. In a complete oscillation there will be four steps, the scanning motion sweeping across both sides of the annulus twice.

This is equivalent to a periodic function of frequency $f_q = 4 f_s$ described by

$$\phi(t) = \begin{cases} 0 & -\frac{1}{4f_q} \leq t \leq \frac{1}{4f_q} \\ \phi_M & \frac{1}{4f_q} \leq t \leq \frac{3}{4f_q} \end{cases}$$

with periodic repetitions.

Letting $f_n = nf_q$ and $K = f_q t$, we have

$$\Phi_0(n) = 0$$

$$\Phi_e(n) = 2\,\phi_M \int_{\frac{1}{4}}^{\frac{3}{4}} \cos 2\pi n K \, dK = \begin{cases} \dfrac{2(-1)^{\frac{n+1}{2}}}{\pi n}\,\phi_M & (n \text{ odd}) \\ 0 & (n \text{ even}) \end{cases}$$

Therefore

$$R_n = \begin{cases} \dfrac{2 r_{f_n}}{n\pi}\,\phi_M & n = \text{odd} \\ 0 & n = \text{even} \end{cases}$$

and

$$R = \frac{2\phi_M}{\pi} \sum_{n=\text{odd}}^{\infty} \frac{r_{f_n}}{n}$$

For the same parameters as in Part I of the report, but remembering we are concerned with f_q, not f_s, we have

$$R = 0.16\,\phi_M$$

Thus a considerable part of the signal is in the good reception region.

We may then expect as an upper limit, radiation from the spike of 5×10^{-7} effective watts/cm². It is certain to be much less than this, as $\phi(t)$ is substantially smoother than a step function. This smoothing is due to the source not being concentrated at the tip of the spike and the presence of the aforementioned bands at the edges of the annulus over which a point source does not fully irradiate the detector. Again, it is to be remembered that if the hot section is small ϕ_M will be smaller than mentioned here. The actual signal can be expected to be at least ten times smaller than the 5×10^{-7} effective watts/cm² derived above.

E. CONCLUSIONS

As in the case of the time-dependent radiation from windows, the signal level from the spike will generally have only a small component at the chopping frequency. It is assumed, however, that the emissivity of the spike is low and that the chopping frequency is well separated from the scanning frequency with only chopping-frequency signals passed by the amplifying system. The emissivity of the spike is discussed at length in Appendix A.

Appendix B gives an analysis of the radiation from partially transparent slabs having a temperature gradient. Here we find that the radiation is greater in the direction of the gradient. This asymmetry in radiation changes the results of the calculation of spike emissivity given in Appendix A. This correction, which corresponds to the energy transfered by conduction is usually neglected. In any given case its magnitude can be found by comparing the power transfered by conduction to that radiated.

To minimize the radiation from the spike, it should be of low emissivity and as thin as possible. It must, however, withstand the aerodynamic loads and high temperatures encountered in flight. The selection of optimum material optimum shape, with possibly the introduction of a coolant into a hollow spike presents an engineering problem with many practical solutions. It is even possible to design an optical system which will never see the spike. Such an arrangement is described in Appendix C.

APPENDIX A
EMISSIVITIES OF CYLINDERS

Here we shall present calculations for the directional emissivity of both dielectric and metallic radiators with circular cross-section. We include the effect of multiple reflections for the general cylindrical case which, at present, does not appear in the literature. McMahon, Ref. 5, treats multiple reflection for an infinite plane slab in the normal direction, while a paper by R. Gardon, Ref. 6, extends McMahon's results in all directions for a plane-parallel slab.

The cylinder under investigation is of infinite length, has radius, a, and is characterized by volume emissive power $\frac{1}{4\pi}$ j(λ, T); i.e., the intensity of radiation emitted by 1 cm^2 of material of thickness dx into a differential solid angle dΩ is j(λ, T) dx dΩ. The absorption coefficient is k(λ, T).

The cylinder has an optically smooth surface, so we can apply the usual boundary conditions for the Maxwell equation ($\lambda << a$) which result in Snell's Law and the Fresnel coefficients between incident, reflected and refracted amplitudes.

It follows from Snell's law that for a given direction of radiation there is a unique cross-section in the cylinder from which the radiation emanates. The intersection of the cylinder by the plane (determined by the radiation ray and a ray normal to the cylindrical surface) is the desired cross-section. This cross-section takes on only three shapes: rectangular, circular and elliptical. We shall treat them first separately and later give a general formula embracing all three cases.

A. RECTANGULAR CROSS-SECTION

The previous treatment of this case was by McMahon and recently by Gardon. McMahon has considered only radiation normal to the slab; while Gardon gave a general treatment for all angles of emission θ. Our intermediate results differ, but that is due to different definitions of intensity.

$$I_s(\theta) = \frac{j}{2k} \frac{(1 - r_s)\{1 - \exp(-2ank/\sqrt{n^2 - \sin^2\theta})\}}{1 - r_s \exp(-2ank/\sqrt{n^2 - \sin\theta}}$$

$$I_p(\theta) = \frac{j}{2k} \frac{(1 - r_p)\{1 - \exp(-2ank/\sqrt{n^2 - \sin^2\theta})\}}{1 - r_p \exp(-2ank/\sqrt{n^2 - \sin\theta})}$$

Tht total intensity is $I = I_p + I_s$ and the degree of polarization $= \dfrac{I_s - I_p}{I_s + I_p}$ r_p and r_s are the reflection coefficient for the material.

These results are plotted in Figs. 9 and 10 with the following values used

$n = 1.5$
$k = 0.1/\text{cm}$

In Fig. 9 we have two plots for thickness $2a = 0.5$ cm and $2a = 1.016$ cm and in Fig.10 we have similar results for an opaque slab, essentially for a slab with $a \to \infty$

According to our definition, if the emitting body obeyed Lambert's law, we would have just a straight horizontal line. The deviation from the straight line thus gives as the deviation from Lambert's law.

For a slab of finite thickness there will be a maximum for the intensity emitted at some θ_0 which is a function of the thickness. This results from the competition of several factors; namely the reflection coefficient which is a function of θ and the exponential in the numerator and denominator.

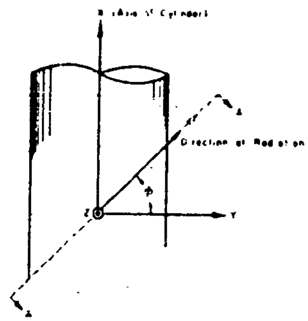

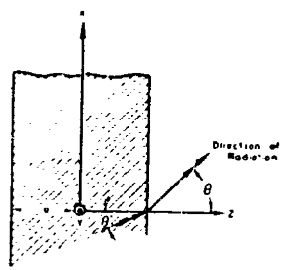

A-A (when $\phi = 0$)

B. CIRCULAR CROSS-SECTION

In a similar manner we can calculate the radiation coming out at the rim of a circle.

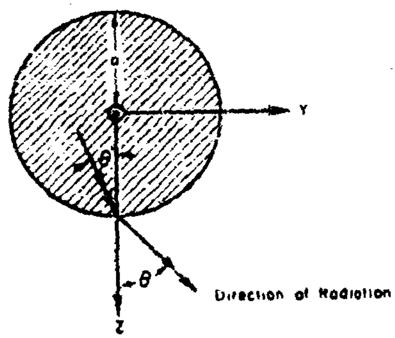

A - A (when $\phi = 90°$)

The length of the optical path is $2a \cos\theta'$ and as a result the radiation emanating at the surface (without multiple reflections) is

$$\frac{1}{k}\left\{1 - e^{-k2a\cos\theta'}\right\}\left\{1 - R(\theta')\right\}$$

and similarly to the infinite plane slab the result including reflected radiation is

$$\frac{1}{k}\;\frac{\left\{1 - e^{-k2a\cos\theta'}\right\}\left\{1 - R(\theta')\right\}}{1 - e^{-k2a\cos\theta'}\,R(\theta')} = \frac{1}{k} = E(\theta')$$

This result is obvious for values of θ' such that it takes an infinite path till we get a closed polygon but it also holds true for $\theta' = \frac{\pi}{4}, \frac{\pi}{6} \ldots$ i.e., when we can inscribe a closed polygon of which the ray under consideration is one side of the polygon.

Proof

Let there be an n-sided polygon. Then the contribution from the i-th side of the polygon ($i = 1, 2 \ldots n$) reaching P for the first time is

$$\frac{j}{k}\left\{1 - e^{-2ak\cos\theta'}\right\}\left\{1 - R(\theta')\right\}\left\{e^{-2ak\cos\theta'} R(\theta')\right\}^{i-1}$$

and for the m-th time around ($m = 1, \ldots \infty$) is

$$\frac{j}{k}\left\{1 - e^{-2ak\cos\theta'}\right\}\left\{1 - R(\theta')\right\}\left\{e^{-2ak\cos\theta'} R(\theta')\right\}^{m(i-1)}$$

Summing this

$$\sum_{m=0}^{\infty}\sum_{i=1}^{n}\frac{j}{k}\{1 - e^{-2ak\cos\theta'}\}\{1 - R(\theta')\}\{e^{-2ak\cos\theta'} R(\theta')\}^{m(i-1)}$$

$$= \sum_{n=0}^{\infty}\frac{j}{k}\{1 - e^{-2ak\cos\theta'}\}\{1 - R(\theta')\}\{e^{-2ak\cos\theta'} R(\theta')\}^{n}$$

$$= \frac{j}{k}\,\frac{\{1 - e^{-2ak\cos\theta'}\}\{1 - R(\theta')\}}{1 - e^{-2ak\cos\theta'} R(\theta')} \quad \text{Q.E.D.}$$

In this case the result is similiar to the infinite plane except that the length of an unbroken path is bounded by the diameter of the circle.

$$I_p(\theta) = \frac{j(\lambda, T)}{2k(\lambda, T)}\;\frac{(1 - r_p)\{1 - \exp(-2ak\sqrt{n^2 - \sin^2\theta}/n)\}}{1 - r_p\exp(-2ak\sqrt{n^2 - \sin^2\theta}/n)}$$

$$I_s(\theta) = \frac{j(\lambda, T)}{2k(\lambda, T)}\;\frac{(1 - r_s)\{1 - \exp(-2ak\sqrt{n^2 - \sin^2\theta}/n)\}}{1 - r_s\exp(-2ak\sqrt{n^2 - \sin^2\theta}/n)}$$

C. ELLIPTICAL CROSS-SECTION

For a thin slab of elliptical shape the inclusion of multiple reflection becomes extremely difficult so we compute only the contribution of the first path which is

$$\frac{1}{k}\left\{1 - e^{\frac{2ak\,(1 + m^2)\sqrt{1 + \tan^2\theta'}}{1 + m^2\,(1 + \tan^2\theta')}}\right\}\left\{1 - R(\theta')\right\}$$

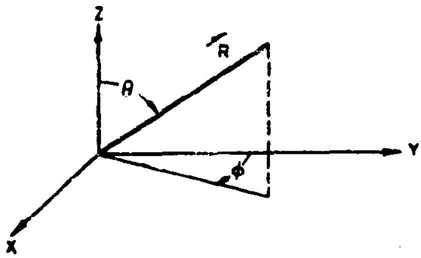

Suppose we observe radiation emitted in the direction $\vec{R}$. Since by our assumption about the nature of the surface Snell's law is obeyed, the radiation will emerge from the cross-section of the cylinder cut by the plane through the Z-axis and $\vec{R}$. Clearly this cross-section will be an ellipse whenever $\phi \neq 0$ or $\phi \neq \frac{\pi}{2}$.

Let's rotate the coordinate axes through Z such that $\phi' = 0$; i.e., Y' coincides with the projection of $\vec{R}$ on the x-y plane.

The equation of this ellipse will be

$$\frac{(z + a)^2}{a^2} + \frac{m^2\,y'^2}{a^2\,(1 + m^2)} = 1$$

where $m \equiv \tan\phi$. The cross-section will have the following shape

$$s = \frac{2a\,(1 + m^2)}{1 + m^2\,(1 + k^2)}\sqrt{1 + k^2}$$

$k \equiv \tan\theta'$

The result is

$$f'(\theta) = \frac{j(\lambda, T)}{k(\lambda, T)} \quad (1 - R) \quad [\, 1 - e^{-k(\lambda, T)s} \,]$$

the prime on $f'(\theta)$ is to denote that this result is the zeroth approximation to the final, extrapolated result as given in the subsequent formula.

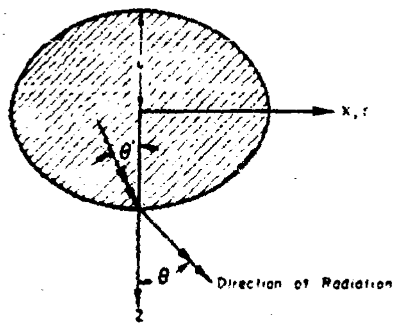

A-A (when $0 < \phi < 90°$)

Here we could only get the emitted intensity without reflection. This result is

$$\hat{f}_p(\theta) = \frac{j(\lambda, T)}{2k(\lambda, T)} \; \frac{(1 - r_p)\left\{1 - \exp\left[\dfrac{-2a\,(1 + \tan^2\phi)\, n\sqrt{n^2 - \sin^2\theta}}{n^2 - \sin^2\theta + n^2\tan^2\phi}\right]\right\}}{1 - r_p \exp\left[\dfrac{-2ak\sqrt{n^2 - \sin^2\theta}}{n}\right]}$$

$$\hat{f}_s(\theta) = \frac{j(\lambda, T)}{2k(\lambda, T)} \; \frac{(1 - r_s)\left\{1 - \exp\left[\dfrac{-2a\,(1 + \tan^2\phi)\, n\sqrt{n^2 - \sin^2\theta}}{n^2 - \sin^2\theta + n^2\tan^2\phi}\right]\right\}}{1 - r_s \exp\left[\dfrac{-2ak\sqrt{n^2 - \sin^2\theta}}{n}\right]}$$

We shall find it convenient, however, to use an empirical expression for the elliptical case including multiple reflection. The justification for this procedure lies not so much in the fact that our expression reduces to the right limit at $\phi = \frac{\pi}{2}$, $\phi = 0$, i.e., for the rectangular and the circular case respectively, but much more in the fact that the difference between the approximate and true result is small anyway for the particular values of k, n which are of interest. So we can write our empirical result

$$f_p(\theta) = \frac{j}{2k}\;\frac{(1 - r_p)\left\{1 - \exp\left[\dfrac{-2a\,(1 + \tan^2\theta)\,n\sqrt{n^2 - \sin^2\theta}}{n^2 - \sin^2\theta + n^2\tan^2\theta}\right]\right\}}{1 - r_p\;\exp\left[\dfrac{-2a\,(1 + \tan^2\theta)\,n\sqrt{n^2 - \tan^2\theta}}{n^2 - \sin^2\theta + n^2\tan^2\theta}\right]}$$

$$f_s(\theta) = \frac{j}{2k}\;\frac{(1 - r_s)\left\{1 - \exp\left[\dfrac{-2a\,(1 + \tan^2\theta)\,n\sqrt{n^2 - \sin^2\theta}}{n^2 - \sin^2\theta + n^2\tan^2\theta}\right]\right\}}{1 - r_s\;\exp\left[\dfrac{-2a\,(1 + \tan^2\theta)\,n\sqrt{n^2 - \sin^2\theta}}{n^2 - \sin^2\theta + n^2\tan^2\theta}\right]}$$

D. TOTAL RADIATION FROM CYLINDER

So far we have gotten expressions for the intensity for the three different cross-sections. However, we would like to have an expression which is valid for any one of the cross-sections. As will be shown later this result is needed if we want to calculate the intensity of parallel rays emerging at a given angle. We propose an expression of the form

$$F(\theta) = \frac{j(\lambda, T)}{2k(\lambda, T)}\;\frac{(1 - R)\,\{1 - e^{-s\,k(\lambda, T)}\}}{\{1 - R\,e^{-sk(\lambda, T)}\}}$$

where $F(\theta)$ stands for either $f_r(\theta)$ or $f_s(\theta)$ and R stands for either r_r or r_s. And

$$s = \frac{2a\,(1 + \tan^2\phi)}{1 + \tan^2\phi\,\sec^2\theta'}\;\sec\theta'$$

$$= \frac{2a\,(1 + \tan^2\phi)}{n^2 - \sin^2\theta + n^2\tan^2\phi}\;n\sqrt{n^2 - \sin^2\theta}$$

$$= \frac{2a\,(1 + \tan^2\phi)}{(n^2 - \sin^2\theta) + n^2\tan^2\phi}\;n\sqrt{n^2 - \sin^2\theta}$$

We shall show that the above expression has the right limit for $\phi = 0$ and $\phi = \frac{\pi}{2}$; i.e., when the cross-section is either rectangular or circular.

a) When $\phi = 0$, $\tan^2 \phi = 0$ and

$$S = \frac{2\,an}{\sqrt{n^2 - \sin^2\theta}}$$ in agreement with our previous results.

b) When $\phi = \frac{\pi}{2}$ then we can neglect 1 with respect to $\tan^2\phi$ and $(n^2 - \sin^2\theta)$ with respect to $n^2 \tan^2\phi$, so that the limit is $\frac{2a}{n}\sqrt{n^2 - \sin^2\theta}$ in agreement with our previous results.

We may then calculate the intensity emanating from cylinder per unit length and into an infinitesimally small solid angle $d\Omega$ at angle θ with the Z-direction. In the usual definition intensity is defined as

$$I = \lim_{\substack{d\sigma \to 0 \\ d\omega \to 0}} \frac{W}{d\sigma\, dt\, d\omega\, \cos\theta}$$

where θ is measured from the normal to the emitting and traversed area $d\sigma$. We generalized this definition somewhat so as to meet our present requirements. We first evaluate the total energy radiated by the bundle of rays in the γ direction and into a solid angle $d\omega$ (this is where the factor $\cos\theta \cos\psi$ enters later into the integrand), and then divide by $\cos\theta$. This definition can be stated symbolically as

$$I_{p,s} = \lim_{d\omega \to 0} \frac{'W'}{d\omega\, \cos\theta}$$

where 'W' is the power radiated by the cylinder across the upper or lower half per unit length. This definition is somewhat artificial but very useful in our applications.

To clarify the problem, we draw the following diagram

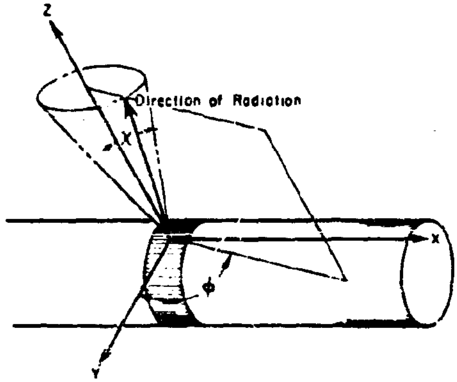

In order to perform the integration we have to express the direction cosines of each ray in a transformed coordinate system Z', Y, X' where the normal to the cylinder at the point where a given ray emerges is the new Z' axis. That is, for each ray we rotate the coordinate system around the x-axis through an angle ψ.

The angles θ, and ϕ used in our formula for S are related to the direction cosines in the following way:

$$\tan\phi = \frac{\cos\alpha}{\cos\beta} \quad ; \quad \cos\theta = \cos\gamma$$

where

$$\cos\alpha = \frac{y - y'}{|R|} \quad ; \quad \cos\beta = \frac{x - x'}{|R|} \quad ; \text{ and } \cos\gamma = \frac{z - z'}{|R|}$$

Next we need an expression for the change of direction cosines due to the rotation.

Writing the rotation matrix we get

$$\begin{vmatrix} \cos\psi & 0 & -\sin\psi \\ 0 & 1 & 0 \\ \sin\psi & 0 & \cos\psi \end{vmatrix} \begin{vmatrix} 0 \\ \cos 20^\circ \\ \cos 70^\circ \end{vmatrix} = \begin{vmatrix} \cos\alpha' \\ \cos\beta' \\ \cos\gamma' \end{vmatrix}$$

$$\cos \alpha' = -\sin\psi\,(\cos 70°)$$

$$\cos \beta' = \cos 20°$$

$$\cos \gamma' = \cos\psi\,(\cos 70°)$$

Therefore

$$\cos \theta = (\cos 70°)\cos\psi$$

$$\tan \phi' = -\sin\psi\,(\cot 70°)$$

As a result we have the integrals on the following page.

$$\int f_p(\theta)\cos A\,dA = \frac{f(\lambda,T)\,a}{k(\lambda,T)\,\gamma}\int_0^{\pi/2}\frac{\left\{1-\left[\dfrac{\gamma\cos\psi-\sqrt{n^2-1+\gamma^2\cos^2\psi}}{\gamma\cos\psi+\sqrt{n^2-1+\gamma^2\cos^2\psi}}\right]^2\right\}\left\{1-\exp\left[-\dfrac{(2ak(1+\delta^2\sin^2\psi)\,n\sqrt{n^2-1+\gamma^2\cos^2\psi})}{n^2\delta^2\sin^2\psi+(n^2-1+\gamma^2\cos^2\psi)}\right]\right\}}{\left\{1-\left[\dfrac{\gamma\cos\psi-\sqrt{n^2-1+\gamma^2\cos^2\psi}}{\gamma\cos\psi+\sqrt{n^2-1+\gamma^2\cos^2\psi}}\right]^2\exp\left[-\dfrac{(2ak(1+\delta^2\sin^2\psi)\,n\sqrt{n^2-1+\gamma^2\cos^2\psi})}{n^2\delta^2\sin^2\psi+(n^2-1+\gamma^2\cos^2\psi)}\right]\right\}}\,\gamma\cos\psi\,d\psi$$

$$\int f_s(\theta)\cos A\,dA = \frac{f(\lambda,T)\,a}{k(\lambda,T)\,\gamma}\int_0^{\pi/2}\frac{\left\{1-\left[\dfrac{n^2(1-\gamma\cos\psi)-\sqrt{n^2-1+\gamma^2\cos^2\psi}}{n^2(1+\gamma\cos\psi)-\sqrt{n^2-1+\gamma^2\cos^2\psi}}\right]\right\}\left\{1-\exp\left[-\dfrac{(2ak(1+\delta^2\sin^2\psi)\,n\sqrt{n^2-1+\gamma^2\cos^2\psi})}{n^2\delta^2\sin^2\psi+(n^2-1+\gamma^2\cos^2\psi)}\right]\right\}}{\left\{1-\left[\dfrac{\gamma\cos\psi\,[\gamma\cos\psi-n^2]+n^2-1}{\gamma\cos\psi\,[\gamma\cos\psi+n^2]+n^2-1}\right]^2\exp\left[-\dfrac{(2ak(1+\delta^2\sin^2\psi)\,n\sqrt{n^2-1+\gamma^2\cos^2\psi})}{n^2\delta^2\sin^2\psi+(n^2-1+\gamma^2\cos^2\psi)}\right]\right\}}\,\gamma\cos\psi\,d\psi$$

With these preliminary results we are ready to tackle the central problem; i.e., to calculate the radiation emanating from a radiating cylinder.

We want to calculate the "intensity" of radiation from the upper half of the cylinder per unit length into a given direction.

Let us digress for a while on the meaning of the word "intensity" as applied to this problem. For the sake of convenience, we calculate the energy radiating into $d\Omega$ around the direction θ and divide the results by $\cos\chi$.

Proceeding with the calculation we get

$$F_p(\chi) = \frac{ja}{2k}\int_0^{\pi/2} \frac{(1-\rho(\chi,\psi))(1-e^{-\beta(\chi,\psi)})}{(1-\rho(\chi,\psi)\,e^{-\beta(\chi,\psi)})}\,d\psi$$

$$F_s(\chi) = \frac{ja}{2k}\int_0^{\pi/2} \frac{(1-\epsilon(\chi,\psi))(1-e^{-\beta(\chi,\psi)})}{(1-\epsilon(\chi,\psi)(e^{-\beta(\chi,\psi)})}\,d\psi$$

$$\alpha = \left\{\frac{\cos\chi\cos\psi - \sqrt{n^2-1+\cos^2\chi\cos^2\psi}}{\cos\chi\cos\psi + \sqrt{n^2-1+\cos^2\chi\cos^2\psi}}\right\}^2$$

$$\beta = \frac{2ak\,(1+\cot^2\chi\sin^2\psi)\,n\sqrt{n^2-1+\cos^2\chi\cos^2\psi}}{n^2\cot^2\chi\sin^2\psi + (n^2-1+\cos^2\chi\cos^2\psi)}$$

$$\epsilon = \left\{\frac{\cos\chi\cos\psi\,[\cos\chi\cos\psi - n^2] + n^2 - 1}{\cos\chi\cos\psi\,[\cos\chi\cos\psi + n^2] + n^2 - 1}\right\}^2$$

The preceding integrals are nothing but a detailed description of the following integrals.

$$I_p = \frac{1}{\cos\chi} \int f_p(\psi) \cos\psi \cos\chi \, dA$$

$$I_s = \frac{1}{\cos\chi} \int f_s(\psi) \cos\psi \cos\chi \, dA$$

We can get the preceding result from these integrals immediately if we recognize the fact that the angles appearing in f_p, f_s which refer to the normal at the point of emission have to be described in terms of the angles of the rotated coordinate system where the normal coincides with Z. This integral can be evaluated numerically. Some results are plotted in Fig. 11.

E. EMISSIVITY OF A METALLIC CYLINDER

The analysis in this case is similar to the dielectric one. As a result of the different boundary conditions we get different expressions for the reflection coefficients. Furthermore in the final expression we can omit the exponential terms because the magnitude of k will attenuate the radiation after the traversal of a wavelength.

The final expressions for the cylinder are

$$I_p = \frac{1}{\cos\chi} \int f_p(\psi) \cos\psi \cos\chi \, dA$$

$$I_s = \frac{1}{\cos\chi} \int f_s(\psi) \cos\psi \cos\chi \, dA$$

$$f_p = \frac{j}{2k} \left\{ \frac{1 - 60\,(\lambda/r_e)\cos^2\chi\cos^2\psi - \frac{2\sqrt{30\lambda}}{r_e}\cos\chi\cos\psi + 1}{60\,(\lambda/r_e)\cos^2\chi\cos^2\psi + \frac{2\sqrt{30\lambda}}{r_e}\cos\chi\cos\psi + 1} \right\}$$

$$f_s = \frac{1}{2k}\left\{\frac{1 - 60\,(\lambda/r_e) - \frac{2\sqrt{30\lambda}}{r_e}\cos\chi\cos\psi + \cos^2\chi\cos^2\psi}{60\,(\lambda/r_e) + \frac{2\sqrt{30\lambda}}{r_e}\cos\chi\cos\psi + \cos^2\chi\cos^2\psi}\right\}$$

where λ is the wavelength of the emitted radiation in cm and r_e is the resistivity of the emitting metal in ohm-cm.

F. RADIATION FROM METALLIC CYLINDERS

The emissivity of a metallic surface as a function of the angle away from the normal is given by the following expressions (Ref. 7).

$$\epsilon_1(\theta) = \frac{1 - 60\,(\lambda/r_e)\cos^2\theta - \frac{2\sqrt{30\lambda}}{r_e}\cos\theta + 1}{60\,(\lambda/r_e)\cos^2\theta + \frac{2\sqrt{30\lambda}}{r_e}\cos\theta + 1}$$

$$\epsilon_2(\theta) = \frac{1 - 60\,(\lambda/r_e) - \frac{2\sqrt{30\lambda}}{r_e}\cos\theta + \cos^2\theta}{60\,(\lambda/r_e) + \frac{2\sqrt{30\lambda}}{r_e}\cos\theta + \cos^2\theta}$$

where λ is the wavelength in cm of the radiation considered and r_e is the resistivity of the material in ohm-cm.

The calculations have been carried out both circular and square metallic cylinders. Wavelength λ was taken as two microns, and resistivity for silver at 900°K was taken to be 5×10^{-6} ohm-cm. The resistivity is an approximate value, since the values published in the "Handbook of Chemistry and Physics" vary from investigator to investigator. Emissivities of other metals are given in Fig. 12. The characteristics of the metal are such that a cylinder of radius one half of the fused quartz cylinder radius will suffice for our purposes; we are able to compare on this basis the radiated intensities of both numerically.

The results (plotted in Fig. 13) show by comparison with Fig. 9 that the total intensity radiated from the metallic cylinder is considerably smaller (at each of the angles 70°, 75°, and 80° calculated) than the total intensity from the dielectric cylinder.

Another conclusion which may be of greater interest is that if we consider the use of a polarizing shield around the object in the dielectric case the intensity will be cut approximately by a factor of 2 while in the metallic case the intensity is reduced by a factor ranging from 18 to 47 going from 70° to 80°.

Offhand it seems strange that this polarizing effect of the metal is not observed in reflected light, but the explanation is fairly obvious. For what it amounts to is that $R_1/R_2 \sim 1$, where R_1 refers to the reflection coefficient of the first component and R_2 refers to the reflection coefficient of the second component, and $1 - R_1/1 - R_2 \approx 20$. Say for the sake of illustration that $R_1/R_2 = 0.9$ and that

$$\frac{1 - R_1}{1 - R_2} = 20$$

Then substituting the first ratio into the second we get

$$R_2 = \frac{19}{19.1}$$

Then if R_1 and R_2 are very close to 1, the ratio $1 - R_1/1 - R_2$ can be much larger than R_1/R_2.

Both dielectric and metallic square cylinders may be considered (Fig. 13) with the result that if only one side is viewed the radiation is smaller than the corresponding radiation emitted from the upper half of a circular cylinder of the same volume. However, if we include the total maximum view, that is two sides of the square cylinder, the total radiation is larger.

We shall now state a theorem which will enable us to tell which of two emitting objects gives the smaller values of IA (I = intensity and A = Area viewed) when the objects have the same volume.

Theorem: Given an emitting object the absorption coefficient of which is different from zero, the smaller A/V is for a given volume, the smaller is the amount radiated.

We shall prove it for a very special case: a slab of material of thickness d and width w, coefficient of reflection R and coefficient of absorption k. Let dw = constant. We have for the radiation emitted in the normal direction per unit length across w into an infinitesimal solid angle an expression

$$F = \frac{w\,(1 - R)\,(1 - e^{-kd})}{1 - Re^{-kd}}$$

The above expression includes multiple reflections.

Differentiating with respect to d and substituting for $w = c/d$ and equating to zero we get

$$0 = \frac{c}{d}\,\frac{(1 - R)}{1 - Re^{-kd}}\left[ke^{-kd} - \frac{1}{d}\,(1 - e^{-kd}) - \frac{Rke^{-kd}(1 - e^{-kd})}{1 - Re^{-kd}}\right]$$

While there may be relative minima for $d < \infty$, at $d \to \infty$ the minimum is absolute. The proof could be generalized for arbitrary shapes and volumes.

As a result, we can clude that for minimum radiation the metallic cylinder should be used.

APPENDIX B

RADIATION FROM PARTIALLY TRANSPARENT SLABS HAVING TEMPERATURE GRADIENTS

We shall consider the following problem here. Given a plane-parallel infinite slab of material with thickness d; by means of external heat baths we keep the two boundaries at different temperatures. As a result of this type of heating we get a temperature distribution inside the material T(x); where $T(0) = T_1$ and $T(d) = T_2$. (See Fig. 1)

Let a beam of light of intensity $I_0(\nu)$ enter the medium normally to the surface. What is the intensity of the emergent beam $I(d, \nu)$ when $T_1 < T_2$ and T_1 is as shown in the diagram and when T_1 and T_2 are interchanged?

We shall assume that T(x) varies slowly enough so that we do not violate local thermodynamic equilibrium conditions too violently.

The equation of transfer one usually writes down for such a problem is

$$\frac{dI_\nu}{dS}(x,y,z,\ell,m,n) = \rho(x,y,z)\left[j_\nu(x,y,z,\ell,m,n) - k_\nu(x,y,z)I_\nu(x,y,z,\ell,m,n)\right]$$

where $\frac{d}{dS} = \left(\ell\frac{\partial}{\partial x} + m\frac{\partial}{\partial y} + n\frac{\partial}{\partial z}\right)$

where ℓ, m, n are the direction cosines. One next makes use of the assumption of "local thermodynamic equilibrium" and puts $j_\nu = k_\nu B_\nu(T)$ (Kirchhoff Law). However this new equation,

$$\frac{dI_\nu}{dS} = \rho k_\nu\left[B_\nu - I_\nu\right] \qquad (1)$$

does not tell the whole story. The above equation does not take into account that $j_\nu(x)$ also depends on the amount of incident intensity at the point x. To remedy this situtation, one works directly with the Einstein coefficients as defined for thermodynamic equilibrium. The result is a modified equation

$$\frac{dI_\nu}{dS} = pk_\nu' \left[B_\nu(T) - I_\nu \right] \tag{2}$$

where $k_\nu' = k_\nu \left[1 - \exp - \frac{h\nu}{kT} \right]$

<u>Solution of the above equation</u>

We limit ourselves to propagation in the normal direction (x direction only) and therefore get a one-dimensional equation. (Actually this restriction is not too unrealistic because the emerging beam will not contain contributions from radiation emitted in directions different from the normal).

So we have to solve the following:

$$\frac{dI_\nu(x)}{dx} = pk_\nu \left[1 - \exp\left(\frac{h\nu}{kT(x)} \right) \right] \left[\frac{2h\nu^3}{c^2} \frac{1}{\exp\left(\frac{h\nu}{kT(x)}\right) - 1} - I_\nu(x) \right] \tag{3}$$

Equation (3) is of the form $\frac{dy}{dx} + yP(x) = Q(x)$ (3)'

where $P(x) = pk_\nu \left[1 - \exp\left(- \frac{h\nu}{kT(x)} \right) \right]$

and $Q(x) = \frac{2h\nu^3 pk_\nu}{c^2} \quad \frac{1 - \exp - \left(\frac{h\nu}{kT(x)} \right)}{\exp\left(\frac{h\nu}{kT(x)}\right) - 1}$

The solution of (3)' is

$$y(x) = \exp\left[- \int_0^x P(S)\,dS \right] \int_0^x \left\{ Q(\eta) \exp\left[\int_0^\eta P(S)\,dS \right] \right\} d\eta$$

If we further specify the initial condition that $y(0) = y_0$ then the solution is:

$$y(x) = \exp\left[-\int_0^x P(S)dS\right]\left[\int_0^x Q(\eta)\exp\left(\int_0^\eta P(S)dS\right)d\eta + y_0\right]$$

or translated into our problem we get

$$I_\nu(x) = \exp\left[-\int_0^x \rho k_\nu\left(1-\exp\left[-\frac{h\nu}{kT(S)}\right]\right)dS\right] \times$$

$$\left\{\int_0^x \frac{2h\nu^3\rho k_\nu}{c^2}\left(\frac{1-\exp\left[-\frac{h\nu}{kT(\eta)}\right]}{\exp\left[\frac{h\nu}{kT(\eta)}\right]-1}\right)\exp\left[\int_0^\eta \rho k_\nu\left(1-\exp\left[-\frac{h\nu}{kT(S)}\right]\right)dS\right]d\eta + I_\nu(0)\right\}$$

Discussion of Results

We wish to compare $I_\nu^{(1)}(d)$ for the case when the beam traverses the slab in the direction of increasing temperature with $I_\nu^{(2)}(d)$ beam traversing slab in direction of decreasing temperature. Without loss of generality we can assume that $T(x) = T_1 + \alpha x$ for case 1 and $T(x) = T_2 - \alpha x$ for case 2

$$I_\nu^{(1)}(d) = \exp\left[-\int_0^d \omega\left(1-\exp\left[-\frac{h\nu}{k(T_1+\alpha x)}\right]\right)dx\right] \times$$

$$\left\{\int_0^d dx'\,\beta\,\frac{1-\exp\left[-\frac{h\nu}{k(T_1+\alpha x')}\right]}{\exp\left[\frac{h\nu}{k(T_1+\alpha x')}\right]-1}\exp\left[\int_0^{x'}\omega\left(1-\exp\left[\frac{h\nu}{k(T_1+\alpha S)}\right]\right)dS\right] + I_\nu(0)\right\}$$

$$\omega = \rho k_\nu$$

$$\beta = \frac{2h\nu^3 \rho k_\nu}{c^2}$$

and $$I_\nu^{(2)}(d) = \exp\left[-\int_0^d \omega\left(1 - \exp\left[-\frac{h\nu}{k(T_2 - \alpha x)}\right]\right)dx\right] \times$$

$$\left\{\int_0^d dx'\,\beta\,\frac{1 - \exp\left[-\frac{h\nu}{k(T_2 - \alpha x')}\right]}{\exp\left[\frac{h\nu}{k(T_2 - \alpha x')}\right] - 1}\quad \exp\left[\int_0^{x'} \omega\left(1 - \exp\left[-\frac{h\nu}{k(T_2 - \alpha S)}\right]\right)dS\right]\right.$$

$$\left. + I_\nu(0)\right\}$$

Let us form the difference

$$I_\nu^{(1)}(d) - I_\nu^{(2)}(d) = \exp\left[-\int_0^d \omega\left(1 - \exp\left[-\frac{h\nu}{k(T_1 + \alpha x)}\right]\right)dx\right] \times$$

$$\left\{\int_0^d dx'\,\beta\,\frac{1 - \exp\left[-\frac{h\nu}{k(T_1 + \alpha x')}\right]}{\exp\left[\frac{h\nu}{k(T_1 + \alpha x')}\right] - 1}\left(\exp\left[\int_0^{x'} \omega\left(1 - \exp\left[-\frac{h\nu}{k(T_1 + \alpha\mu)}\right]\right)d\mu\right] - \right.\right.$$

$$\left.\left. \exp\left[\int_{d-x'}^{d} \omega\left(1 - \exp\left[-\frac{h\nu}{k(T_1 + \alpha\mu)}\right]\right)d\mu\right]\right)\right\}$$

Call $$\frac{1 - \exp\left[-\frac{h\nu}{k(T_1 + \alpha x')}\right]}{\exp\left[\frac{h\nu}{k(T_1 + \alpha x')}\right] - 1} = A(x')$$

and $$\exp\left[\int_0^{x'} \omega\left(1 - \exp\left[-\frac{h\nu}{k(T_1 + \alpha\mu)}\right]\right)d\mu\right]$$

$$- \exp\left[\int_{d-x'}^{d} \omega\left(1 - \exp\left[-\frac{h\nu}{k(T_1 + \alpha\mu)}\right]\right)d\mu\right] = B(x'; d - x')$$

One can easily see the $A(x')$ is decreasing with x' and that $B(x'; d - x')$ is non-negative everywhere. This follows from the fact that $(1 - \exp[-h\nu/k(T_1 + \alpha\mu)])$ is a decreasing function of μ. So it follows that $I^{(1)}(d) - I^{(2)}(d) > 0$.

Now let us ask another question. Do the same conclusions hold if k_ν increases with temperature? Naturally if $k_\nu(x)\ (1 - \exp[-h\nu/k(T_1 + \alpha x)])$ is still a decreasing function then the conclusions are the same.

Next should $k_\nu(x)\ (1 - \exp[-h\nu/k(T_1 + \alpha x)])$ be independent of x, then $I_\nu^{(1)}(d) = I_\nu^{(2)}(d)$.

And the third possibility that

$\frac{d}{dx}\ \{k_\nu(x)\ (1 - \exp[-h\nu/k(T_1 + \alpha x)])\} > 0$, then $I_\nu^{(1)}(d) - I_\nu^{(2)}(d) < 0$

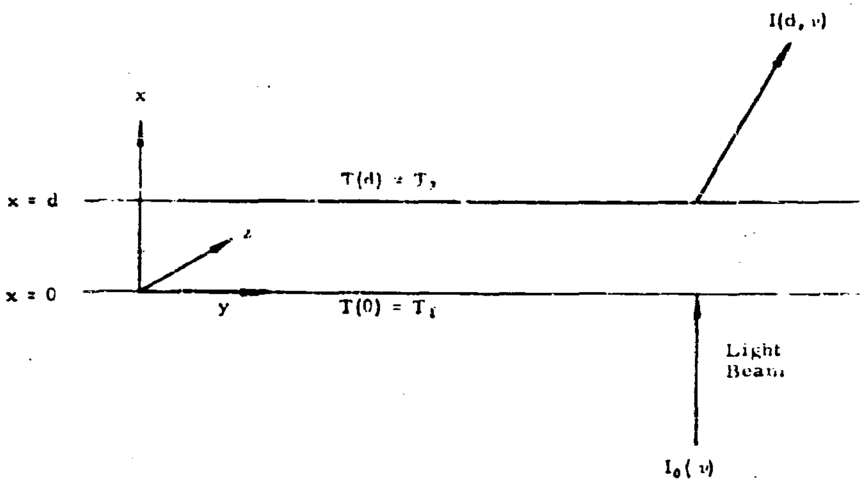

APPENDIX C
INVISIBLE SPIKE

It now remains to consider methods which will conceal the spike from the detector.

There are two possibilities. First, the spike can be angled so as to be hidden by the secondary mirror. Since the angle between the optical axis and the missile axis and the angle of attack of the missile are not related there would then be positions in which the spike would be at too great an angle with respect to the direction of motion for best aerodynamic operation. A better solution is to adjust the optical system so as to mask a spike fixed on the missile; for example, by moving the secondary mirror.

As the optical system is tilted to follow an off-axis target, the physical spike generally comes into the view of the detector, and unless precautions are taken a signal is produced. A simple method of shielding the spike from view, by means of a moving secondary mirror, will be described here.

The primary mirror of the optical system is rotated about the focal point when an off-axis object is to be observed. At the same time the secondary mirror is translated parallel to itself in the plane of its silvered surface. The translation blocks the spike from view. Since the focal point is unchanged and the plane of the secondary mirror is preserved, the radiation is focused at the same point at all times, and hence the detector is left stationary. A slot in the primary permits tilting the primary about the axis of the missile while leaving the detector stationary. The slot may be so placed as to be in line with one of the supports of the secondary, so that no additional information is lost through its presence. Then moving the primary does not produce a signal when different parts of the slot come into the view of the detector.

Using a geometry where the diameter of the aperture is $11\frac{1}{2}$ cm and, the length of the spike 14 cm, (see Fig. 8) one finds that the secondary must cover about 1/4 of the aperture in order for the mirror to shield out the spike for a 20° tilt. This still leaves one with a reasonably high f-number in our flattened cassegrainian system.

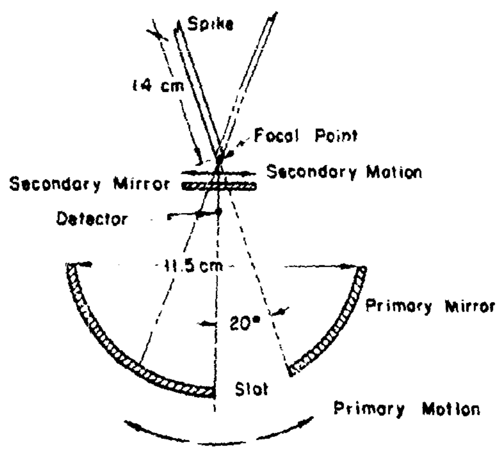

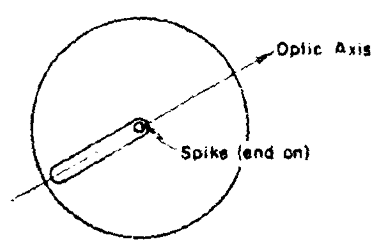

REFERENCES

1. Rubin, E.S., "Resume of Naval Supersonic Laboratory Infrared Effort Reading to a Possible Solution to the "Hot Window Problem", Massachusetts Institute of Technology, Naval Supersonic Laboratory, Report TR 155, December 1955.

2. Schindel, L.H., Covert, E.E., Durgin, F.H., and Rubin, E.S., "An Investigation of the Temperature Distribution on Conical and Hemispherical Infrared-Seeker Windows at Mach numbers 3.0 and 3.5, Part I - Equilibrium Temperatures and Part II - Transient Temperatures", Massachusetts Institute of Technology, Naval Supersonic Laboratory, Wind Tunnel Report numbers 60-1 and 60 [illegible] August 1955.

3. Wilcox, H.A. and Christman, T.J. "Status Report of Sidewinder Program as of 1 August 1953", NOTS TM 1653, USNOTS, Inyokirn, China Lake, California, CONFIDENTIAL

4. Block, Myron J. "Studies Related to Radiation from Hot Windows" Appendix B of 7th Quarterly Progress Report AF-33(616)-2107.... Massachusetts Institute of Technology, Naval Supersonic Laboratory, March, 1955.

5. McMahon, H.O., J. Am. Ceram. Soc. <u>34</u>, 91 (1951)

6. Gardon, R., J. Am. Ceram. Soc. <u>39</u>, 278 (1956)

7. Jakob, M., "Heat Transfer Vol. I", (John Wiley and Sons, New York 1949).

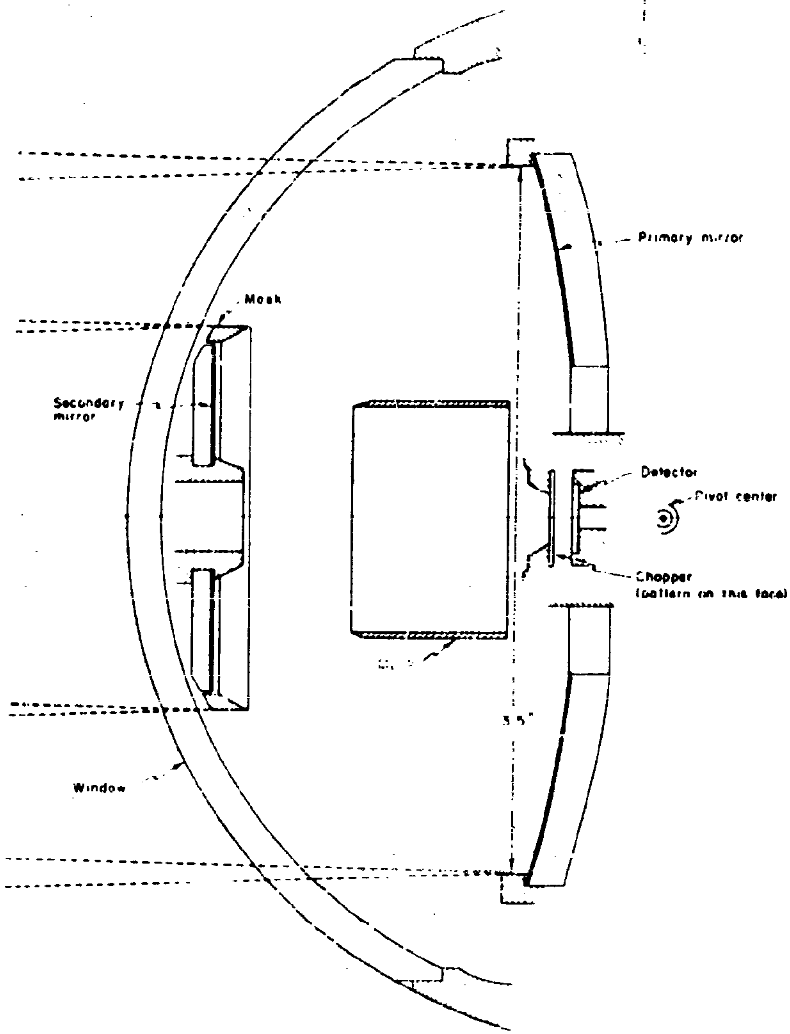

Figure 1: Typical IR Optical System

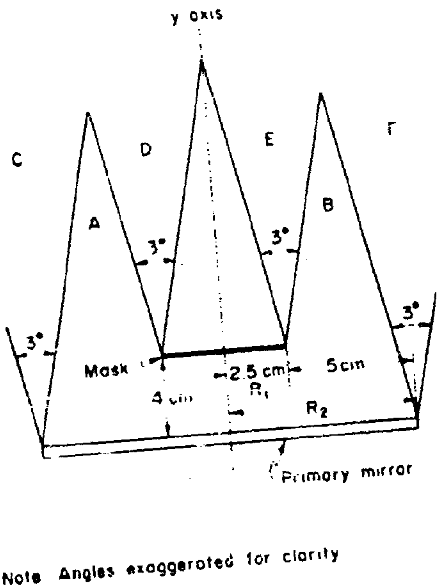

Figure 2. Field of View Divided Using "Conical Construct"

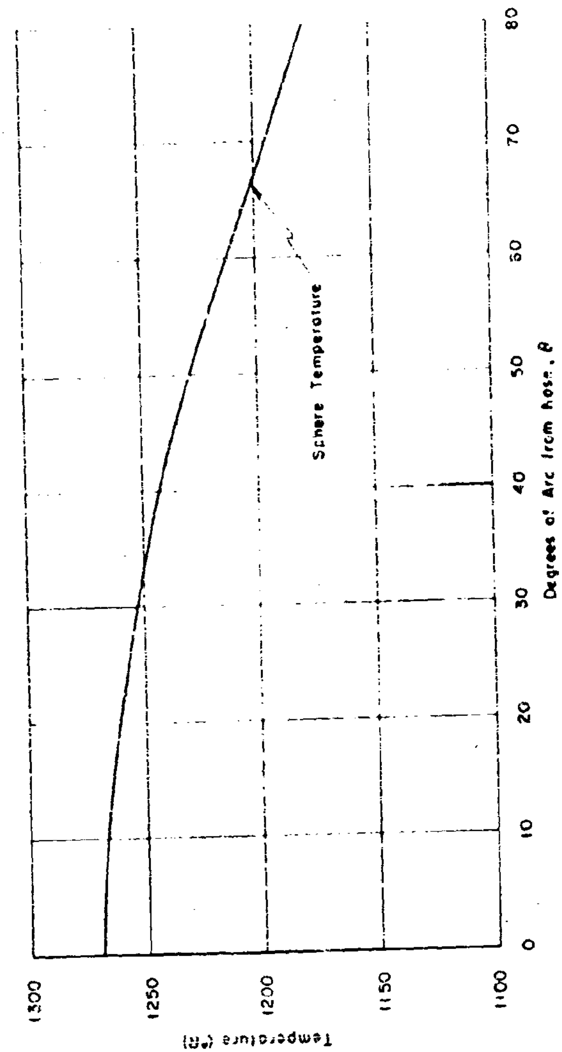

Figure 5. Estimated Temperature Distribution on a Radiating Hemisphere (h = 50,000 ft., M = 3.5)

CONFIDENTIAL

AD 313 752

2 OF 2

FOR
MICRO-CARD
CONTROL ONLY

CONFIDENTIAL

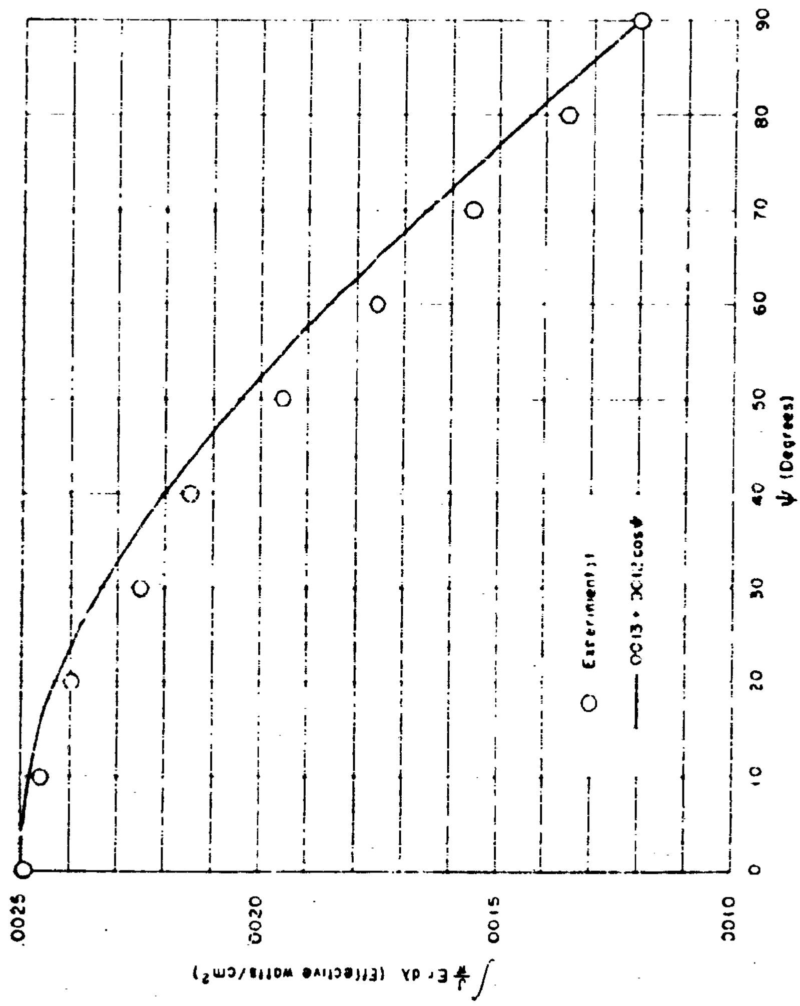

Figure 4. Effective Intensity Distribution on Hemispherical Quartz Window (5mm thick) h = 50,000 ft., M = 3.5

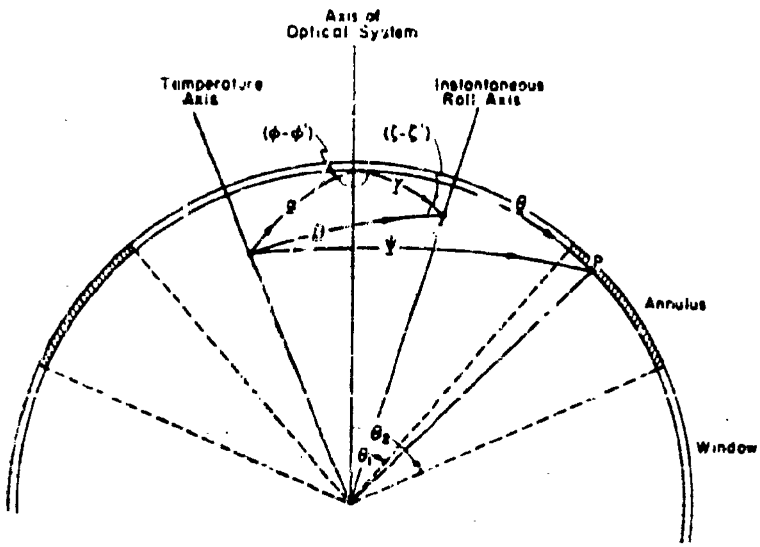

Figure 5. Geometry of Sidewinder Type Window

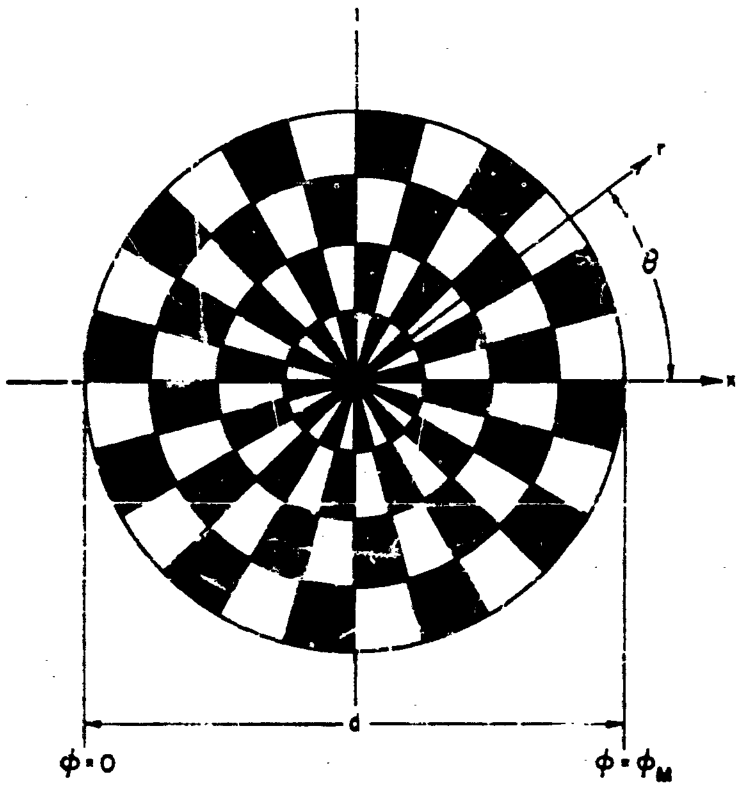

Figure 6. Schematic Diagram of Sidewinder Reticle with Linear Irradiation

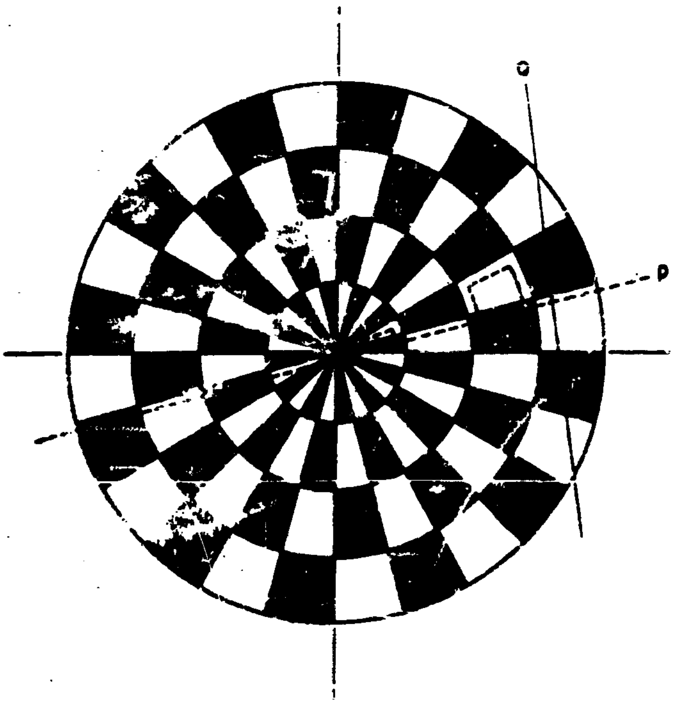

Figure 7. Curves [illegible] Step-Function Variations in Irradiation of [illegible]

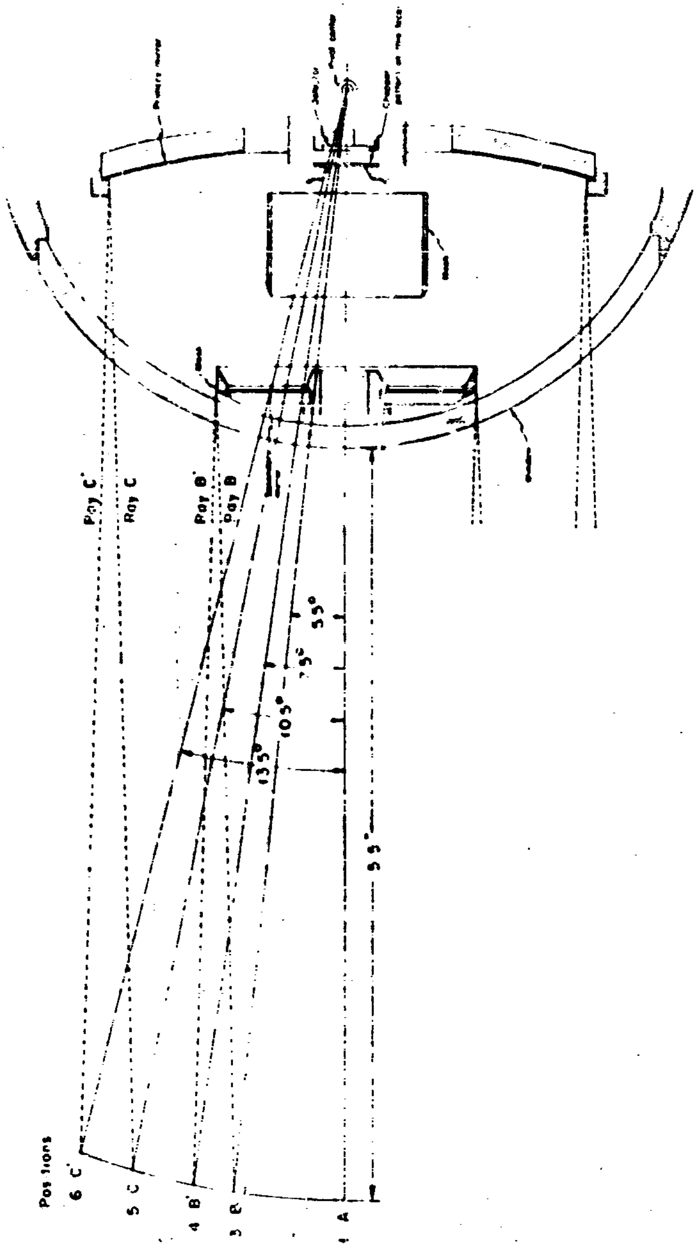

Figure 8. Spike on Sidewinder-Type Detector

CONFIDENTIAL

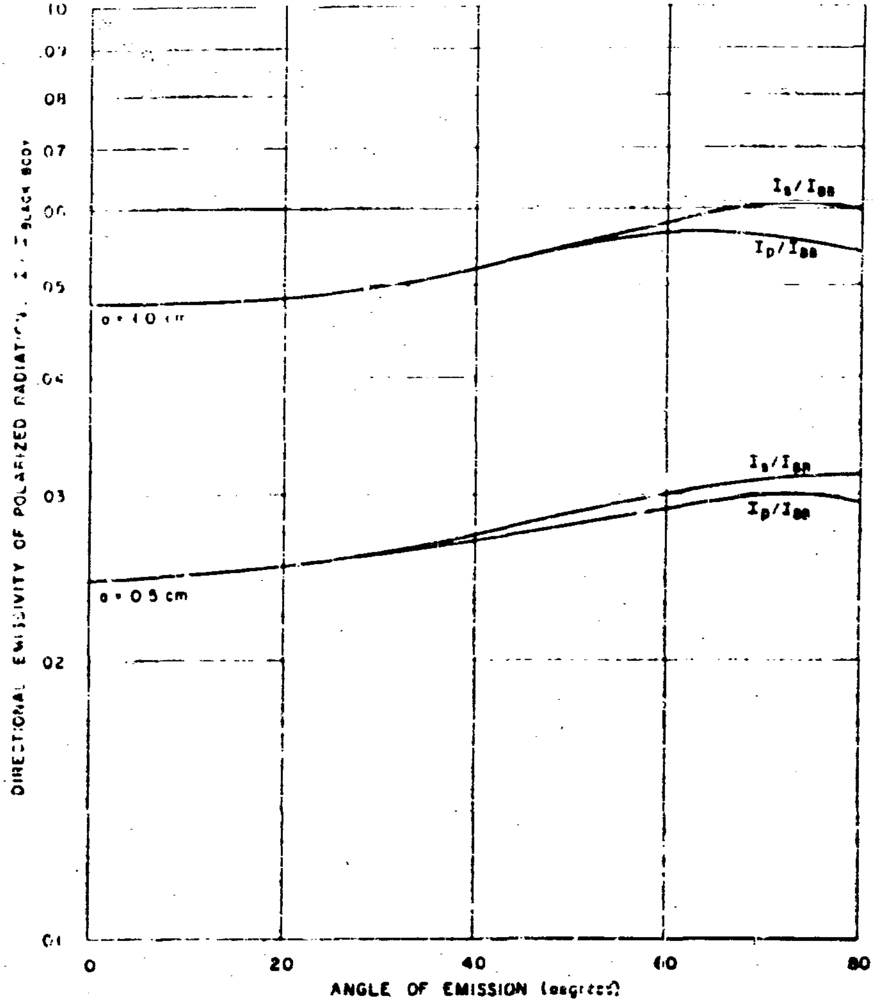

Figure 9. Directional Emissivity of Slab of Width 2a

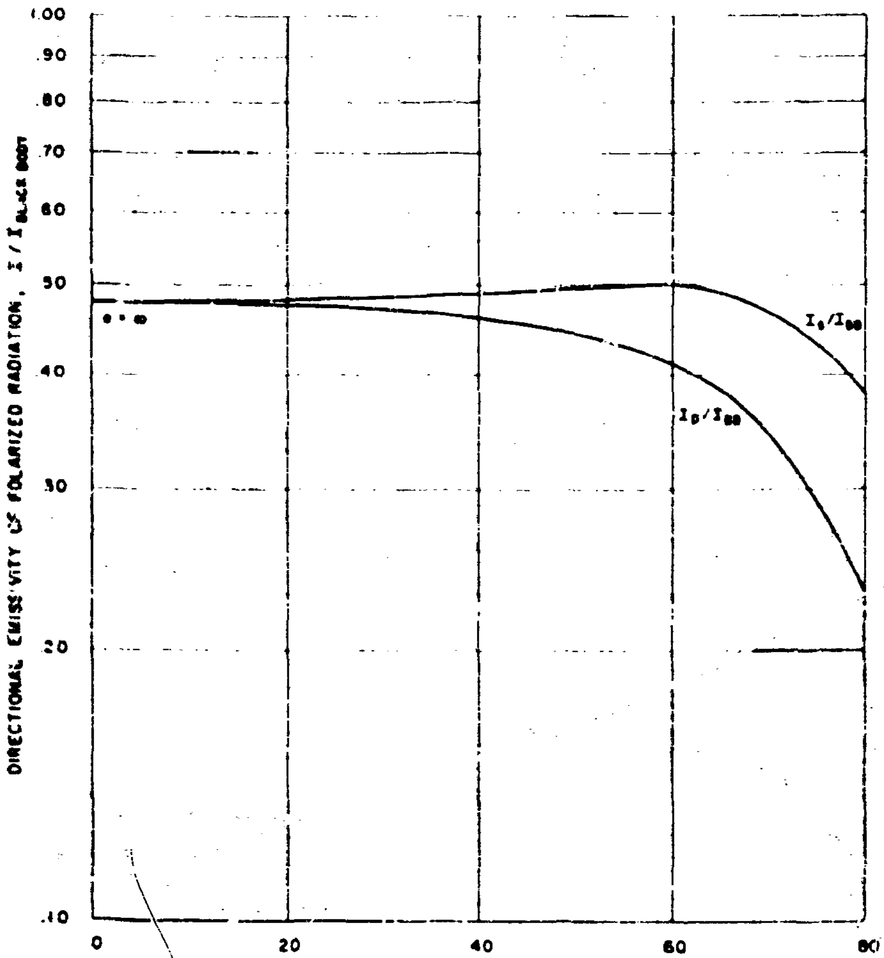

Figure 10. Directional Emissivity of Infinitely Thick Plate

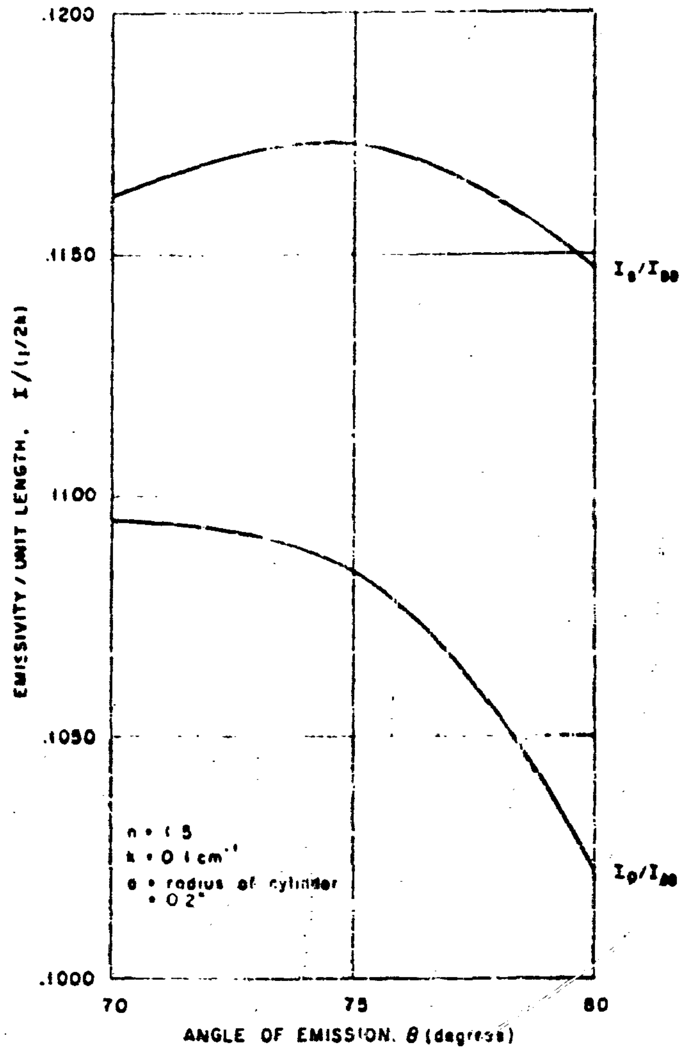

Figure 11. Directional Emissivity of Partially Transparent Dielectric Cylinder

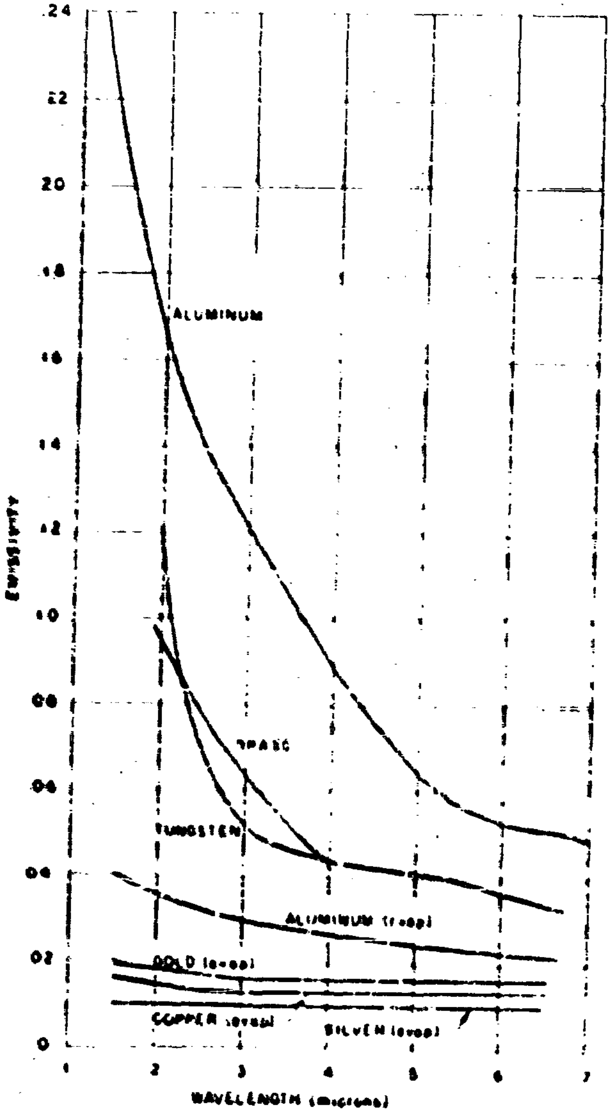

Figure 12. Spectral Emissivity of Metals

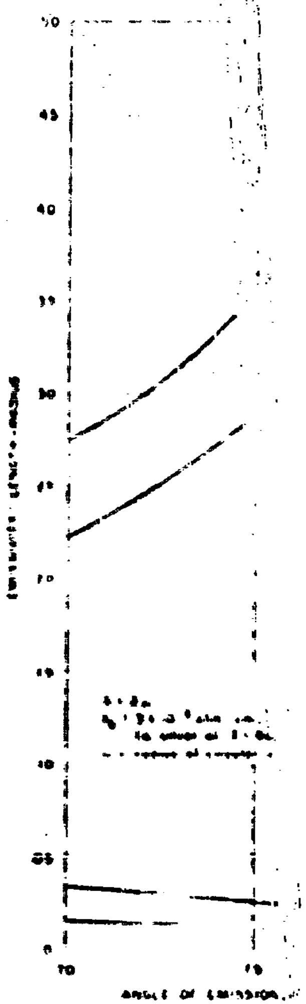

Figure 13. Directional Li

UNCLASSIFIED

UNCLASSIFIED